

NAGI-1318

**The Split Window Microwave Radiometer (SWMR)
for Hurricane Wind Speed Measurement from Space**

Prepared by:

C.T. Swift

University of Massachusetts, Amherst

in collaboration with P. G. Black of
the NOAA Hurricane Research Division

Prepared for:

NASA Langley Research Center

Hampton, VA 23665

Antennas and Microwave Research Branch

GRAN-
11-47-CP
149099
P.38

(NASA-CR-192316) THE SPLIT WINDOW
MICROWAVE RADIOMETER (SWMR) FOR
HURRICANE WIND SPEED MEASUREMENT
FROM SPACE Final Report
(Massachusetts Univ.) 38 p

N93-19987

Unclass

G3/47 0149099

38P

July 27, 1992

Abstract

The monitoring of hurricanes demands considerable resources each year by the National Oceanic and Atmospheric Administration. Even with the extensive use of satellite and airborne probing of those storms, there is still much uncertainty involved in predicting landfall for timely evacuation of people subject to the threat. The concept of the Split Window Microwave Radiometer (SWMR) is to add an additional capability of remotely measuring surface winds to hopefully improve prediction capabilities – or at least define the severity of the storm while it is far from land.

Some of the present science and observational needs are addressed in this report as are remote sensing limitations which impact the design of a minimal system which can be launched into low earth orbit by a low cost launch system. This study has concluded that wind speed and rain rate maps of hurricanes can be generated with an X-Band radiometer system with an antenna whose aperture is 2 m on a side.

INTRODUCTION

The objective of this report is to present science rationale and technical requirements for a potential passive microwave system to monitor hurricanes and tropical storms from low earth orbit. By measuring ocean surface wind speed and rain rate from the convective rain bands of storms, a multi-year data base will be established to advance our understanding of the genesis of hurricanes. In addition to providing a data base for scientific research, the synoptic monitoring of the wind patterns within the storm will enhance our ability to predict the movement and thereby improve our forecasts for landfall. For years, research has been devoted to studying hurricane dynamics and developing models for forecasting their intensity and path of travel. Much of the attention has been concentrated on the hurricane planetary boundary layer because it is there that convective processes are initiated and where the transport of heat and moisture from the ocean occurs. Since it is the winds at the surface that cause the damage at landfall directly and indirectly via the storm surge, the dynamics of the surface winds are of prime interest to researchers and forecasters.

Present methods for estimating hurricane force surface winds often have limited accuracy. Large scale circulation can be inferred from visible imagery via NOAA GOES; however, limited information can be gleaned on the boundary layer winds. In fact, aircraft penetration at low altitudes are the only present source of surface wind measurements. Estimates derived from aircraft reconnaissance are frequently based on Beaufort state of the sea observations, whose validity for hurricane-force winds has not been established. The sustained flight-level winds at 3300 meters are used to infer surface winds; however, the accuracy of extrapolating the flight-level winds to the surface is not always reliable. To date, the only reliable method of obtaining the surface windspeed has been with low-level penetration of the hurricane by suitably equipped aircraft. This is a hazardous operation because severe turbulence is frequently encountered by the aircraft. In addition, the extent of the storm is such that it is only practical to collect data over a few flight lines, which is far from a synoptic measurement of the hurricane.

With the advent of satellite oceanography, it was recognized that microwave radiometers had the potential of remotely measuring windspeed over the ocean. These systems are responsive to changes in ocean surface windspeed as a result of the change in surface emission due to surface roughness and foam. It is well established that passive microwave emission from the ocean is strongly correlated with surface windspeed Nordberg et al., (1971); Ross and Cardone, (1974); Hollinger, (1971). Webster et al. (1976) find a linear relationship between excess brightness temperature and windspeed irregardless of the choice of electromagnetic frequency, viewing angle, or polarization. For horizontal polarization (electric vector parallel to the surface) there is approximately a 1K increase in brightness temperature for every 1 m/s increase in windspeed. This linear relationship was generated from a data set for windspeeds not exceeding 20 m/s.

Although Webster et al. indicate that microwave radiometers provide an encouraging means of measuring windspeed in a hurricane, there is one major problem that must be addressed. In hurricanes, high winds are almost always associated with heavy rain; e.g., rain rates up to 50 mm/hr. Although microwaves can penetrate clouds to measure signatures of surface phenomenon, rain drops are large enough to present appreciable electromagnetic interaction and will add error to the surface measurement unless a reliable atmospheric correction is somehow applied. It has been proven that the rain signature is a strong function of frequency, whereas, the surface wind speed signature is not.

If near simultaneous data are collected at two or more frequencies, atmospheric and surface effects are separable. Data should be collected at the lowest possible frequency so that rain will only provide weak attenuation so that the surface can be "seen" by the instrument. On the other hand, the frequency should not be too low as to make the antenna prohibitively large. The trade-off of atmospheric penetration vs. antenna size is a major component of this report.

The split window technique is derived from the radiometric concepts developed and demonstrated by the Stepped Frequency Microwave Radiometer (SFMR) and the Push-Broom Microwave Radiometer (PBMR). The SFMR was developed by NASA Langley Research Center (LaRC) during the 1970's (Harrington, 1980). A second SFMR was developed by the Microwave Remote Sensing Laboratory (MIRSL) of the University of

Massachusetts during the 1980's and is presently being flown on NOAA hurricane flights. An L-band multiple-beam microwave radiometer, the PBMR, was developed and flown by NASA LaRC during the 1980's (Lawrence et al., 1984). The PMBR is presently collecting soil moisture data in a joint flight program between LaRC and the Goddard Space Flight Center.

The SFMR was first flown into hurricane Allen in August 1980. During data collection, the SFMR was programmed to sequentially operate at 4.5, 5.0, 5.6 and 6.6 GHz. Sampling occurred within a time period that was short compared to the movement of the antenna footprint along the ocean surface. The Hurricane Allen flights proved that SFMR techniques can clearly differentiate between the eye wall of a hurricane which is associated with heavy rainfall over high winds and the eye itself which is associated with calm winds and no precipitation. Brightness temperatures were relatively warm when windspeeds were high and cold when windspeeds are low. Furthermore, there was strong frequency dependency on the radiometer signature when the rain was present; i.e., the brightness temperature at 6.6 GHz was substantially higher than that at 4.5 GHz, when rain was in the field of view of the sensor. When the apparent rain rate was low, the frequency dependency was much less evident. Other events are discussed by Jones et al. (1981), and Black and Swift (1984). The SFMR results are in good relative agreement with the atmospheric planetary boundary layer mode surface winds over a dynamic range of windspeeds ranging from near 0 m/s in the eye to approximately 70 m/s (140 kts) in the eye wall.

The University of Massachusetts SFMR has flown successfully on the NOAA P-3 during every hurricane season since 1984 (Tanner, Swift, and Black, 1987). The bulk of the activity has consisted of validating the performance of the sensor against more conventional means of measuring windspeed and in refining the algorithm to use an ensemble of six frequencies. To date, there have been no inconsistencies in the winds as derived from the SFMR, and the accuracy has improved to ± 1.4 m/s for windspeeds greater than approximately 20 m/s.

BACKGROUND

A key component of hurricane warnings issued by the National Weather Service's National Hurricane Center (NHC) is the estimation of expected surface winds. Until recently, no reliable means of measuring surface winds in hurricanes over the open ocean prior to its landfall has existed. This problem frequently leads to an over-estimation of surface winds at sea from aircraft flight level reconnaissance observations and an overwarning of surface winds at landfall. Since a preparedness cost of \$50M per storm is incurred an average of twice per year in the United States, considerable savings could be realized if the overwarning area could be reduced by even 10 percent through improved surface wind measurements.

The problem of estimating the expected surface wind at a given location consists of: 1) estimating current surface winds at the initial forecast time and 2) forecasting the track and intensity tendency of the storm. The wind itself is composed of a steady, or mean, component and a fluctuating, or gust, component. The primary source of information for estimating winds in a hurricane is reconnaissance aircraft measurements at one of three typical flight levels: namely 1,500 ft., 5,000 ft (850 mb) or 10,000 ft (700 mb). The present procedure of estimating the steady surface wind from the aircraft data is simply to assume that it is the same as the flight level value, a practice that invariably results in an overestimate. The present practice of estimating the peak gust is to simply add 15 kts to the steady component. The present method used to forecast the wind is to extrapolate the initial estimate into the future using a linear trend of past estimates.

In order to evaluate the potential of remote sensing techniques, a joint activity between the University of Massachusetts and the NOAA Hurricane Research Division (HRD) has been underway since 1984. Measurements have been made in a phased developmental effort, consisting of a demonstration phase, a confirmation phase, and the present implementation phase. In the first phase, a three-frequency instrument was initially built and flown in the 1984 and 1985 hurricane seasons. Experiments during these two years led to an instrument redesign, which applied better calibration procedures, and a re-build of all the

non-microwave circuits. In addition, a circuit was added to automatically cycle the instrument through six-frequencies after aircraft power-up. Also during this phase, a real-time wind speed calculation capability was added, and the resulting observations were manually transmitted through the aircraft to satellite data link (ASDL) to the National Hurricane Center for the first time in 1987. At the end of the 1989 hurricane center, measurements were made on 75 flights into 24 hurricanes without a single instrument failure. Presently, the onboard aircraft computer system provides SFMR derived real-time measurements of rain rate and wind speed. The UMass SFMR is documented in theses by Ryan (1984) and Chandler (1987).

A particularly well documented confirmation of the accuracy of the SFMR derived surface winds was obtained during a hurricane boundary layer experiment in Hurricane Earl on 13 September 1986. On one radial pass centered at the eye, two NOAA WP-3D aircraft were flown simultaneously from eastern periphery of the storm to the center. The aircraft with the SFMR was flying at 5,000 feet, and the other flew at a lower altitude of 1,500 feet. Wind profiles along this track, as measured by onboard sensor, are shown in Figure 1, along with the surface winds as derived by the SFMR. A scatter plot of the SFMR surface winds on flight level winds from the two aircraft are shown in Figure 2, and the results demonstrate that the average surface wind is 75% of the flight level wind with an uncertainty of 9%, and that the root-mean-square (RMS) error is 1.4 m/s, or about 3 kts. Additional verification of the relationship between flight level wind and surface wind as determined from the SFMR has been conducted by comparing surface buoy observations with concurrent aircraft observations over a period of several years. The aircraft/buoy data comparisons are shown in Figure 3. This data, which is independent of the SFMR measurements, leads one to observe: (1) that the mean buoy surface wind is also 75% of the flight level wind for unstable conditions, defined by negative air-sea temperature difference. (2) that the mean surface wind is only 53% of the flight level wind for stable conditions, defined by positive air-sea differences and (3) the gust factor for winds above gale force is 1.23 and is independent of stability, yielding peak gusts that are 95% and 67% of flight level winds for unstable and stable conditions, respectively. These results have consistently been used to convert measured flight winds to surface winds. Unfortunately,

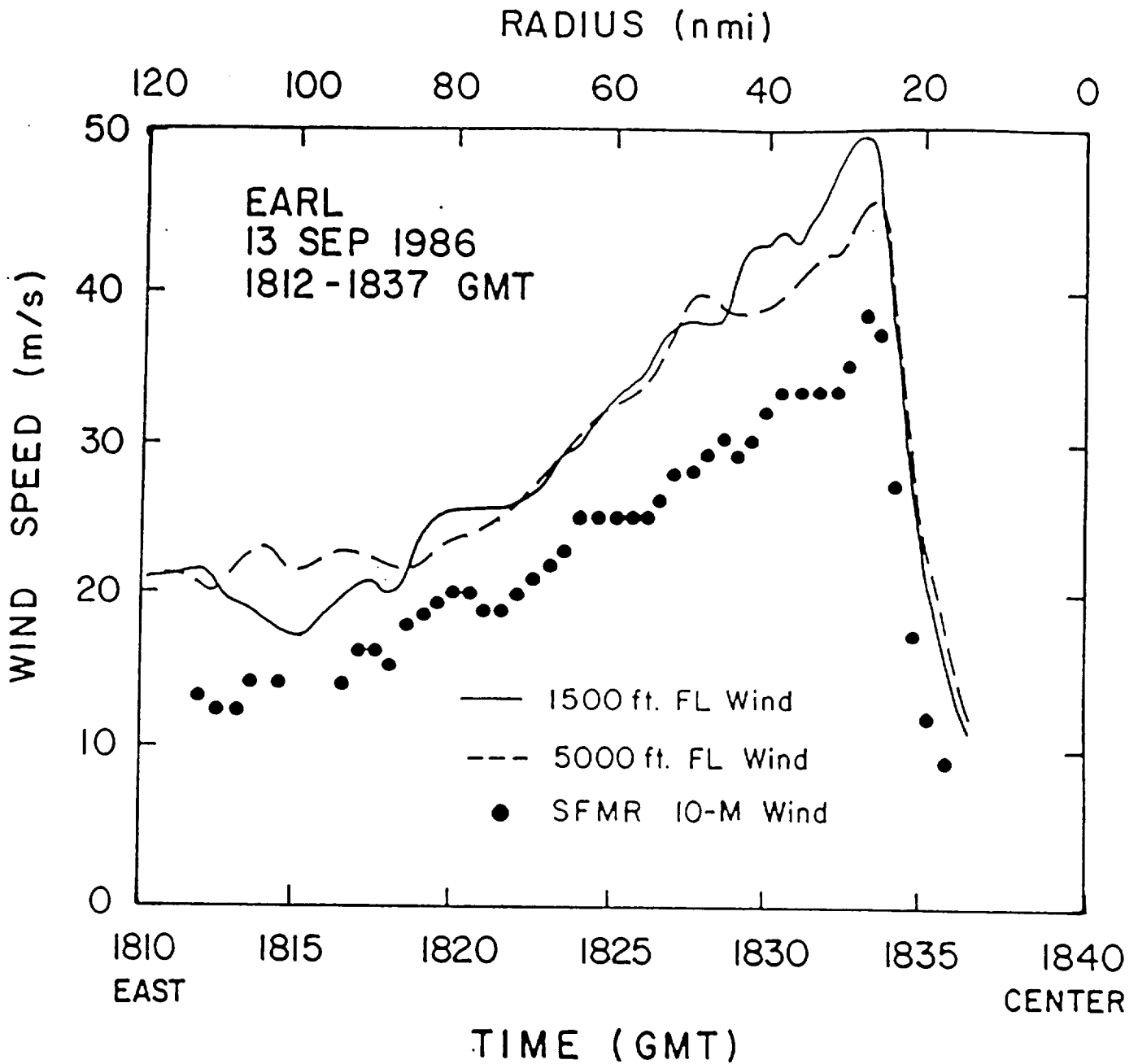


Fig. 1. Flight level wind measurements made simultaneously by two WP-3D's in Hurricane Earl along a flight leg inbound to the eye compared to remotely sensed 10-m surface wind inferred from the Stepped Frequency Microwave Radiometer (SFMR) mounted on the 5000 ft aircraft.

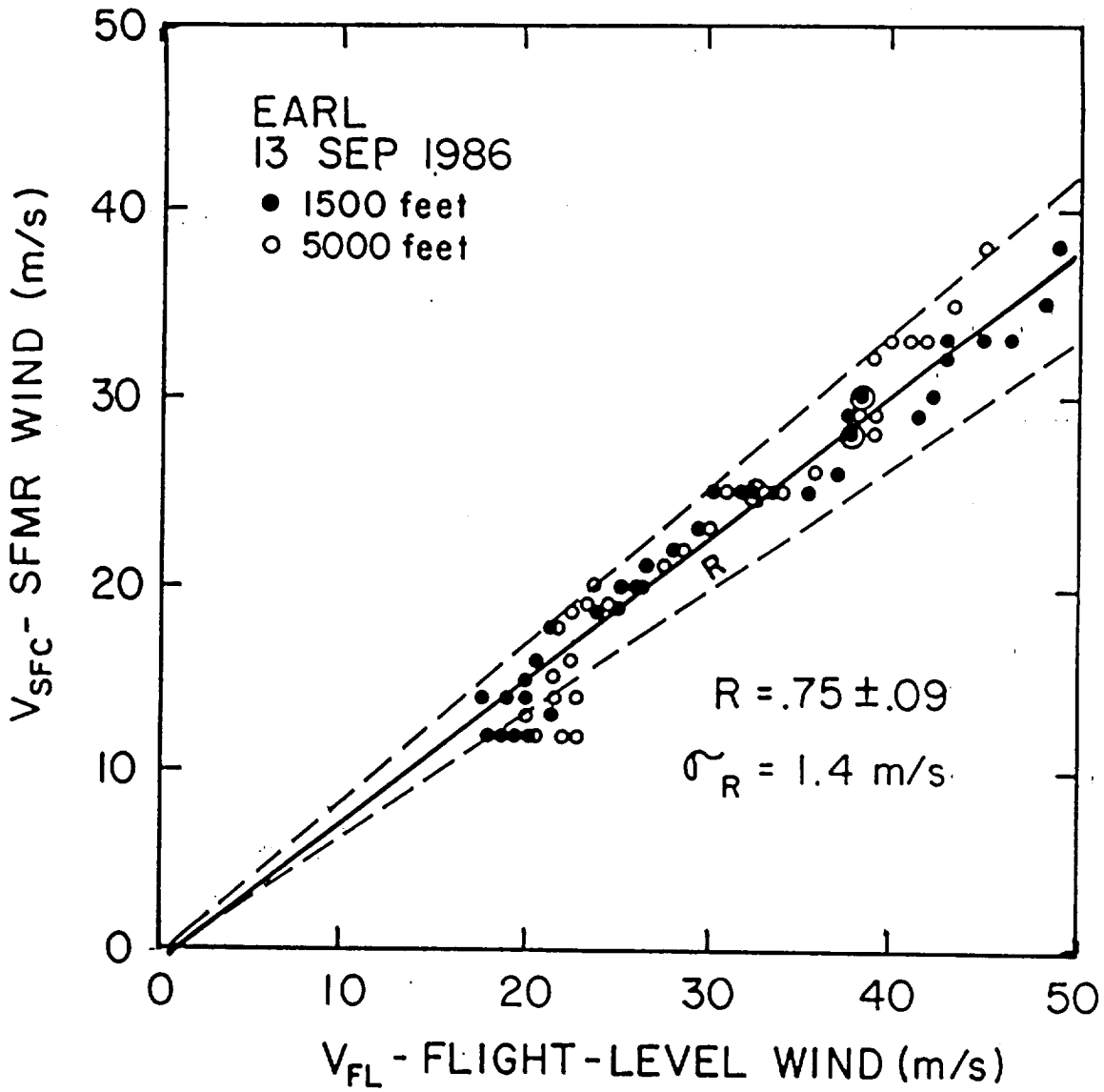
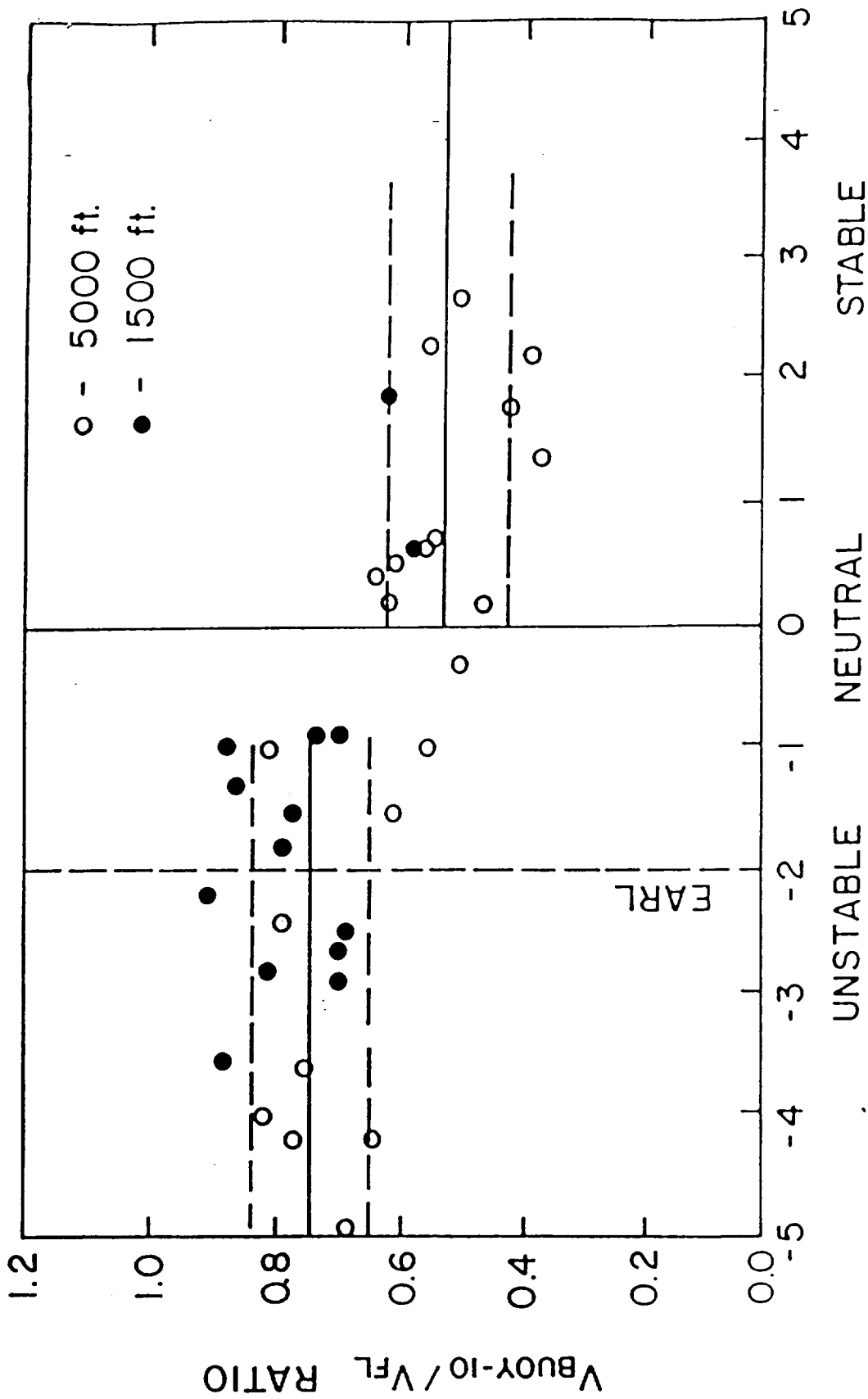


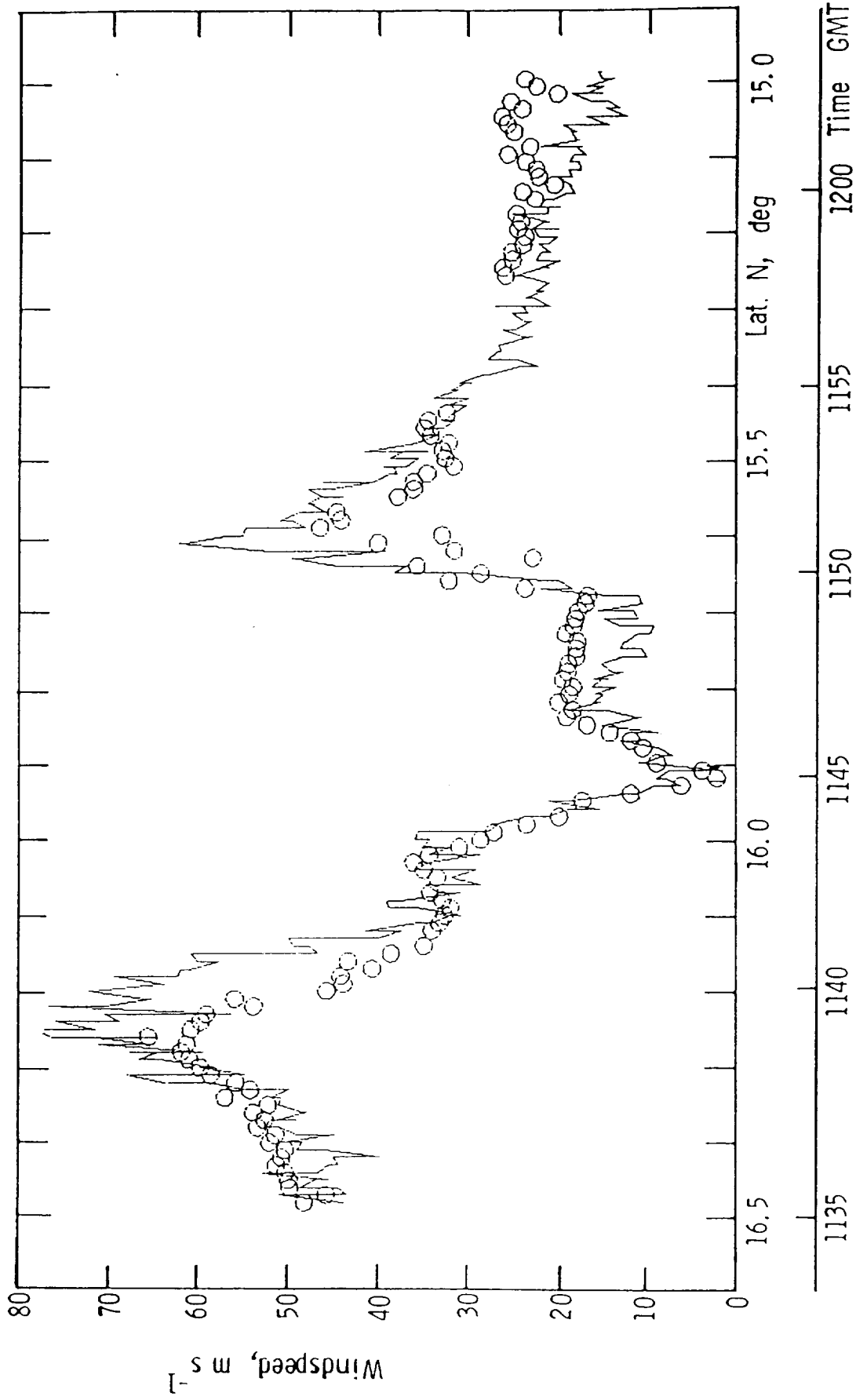
Fig. 2. Scatter diagram of the SFMR winds from Fig. 1 plotted as a function of the flight level winds. The best fit linear regression line with a slope of .75 is shown in red together with the 9% error lines (dashed). Standard deviation about the regression line is 1.4 m/s.



AIR / SEA TEMPERATURE DIFFERENCE (C)

Fig. 3. The ratio of simultaneous measurements of mean 10-m buoy surface wind to flight level wind plotted as a function of boundary layer stability. The mean and standard deviation for unstable and stable conditions is shown by the red solid line and the dashed line, respectively. The solid blue line and error bar is the ratio for 10-m peak gusts. The vertical dashed line indicates the air-sea temperature difference for the Hurricane Earl case in Figs. 1 and 2.

there is considerable uncertainty in determining the actual surface winds, which is lost by the operational people who routinely use these simple scaling factors. In several instances, the SFMR has measured substantial departures from winds derived from these simple scaling factors. The first example was encountered in the very first SFMR flight through Hurricane Allen. Figure 4 shows the winds, as derived from the old retrieval algorithm. The SFMR results (continuous line) are generally consistent with the values determined from the flight level winds (circles). That is to say, the SFMR derived winds are high at the eye walls, and low at the eye. However, the wind speed gradients as measured by the SFMR are significantly different from those derived from the in-situ flight level winds. If the SFMR derived winds are accurate, as we believe they are, then there must be a lateral variation of wind speed as a function of altitude above the surface. This is only one of several examples that we have encountered where the extrapolated flight level winds appear to give erroneous results.



Surface wind speed derived from radiometer brightness temperature (continuous line), and from the low level aircraft (small circles).

FIGURE 4

THE NEED FOR A SATELLITE INSTRUMENT

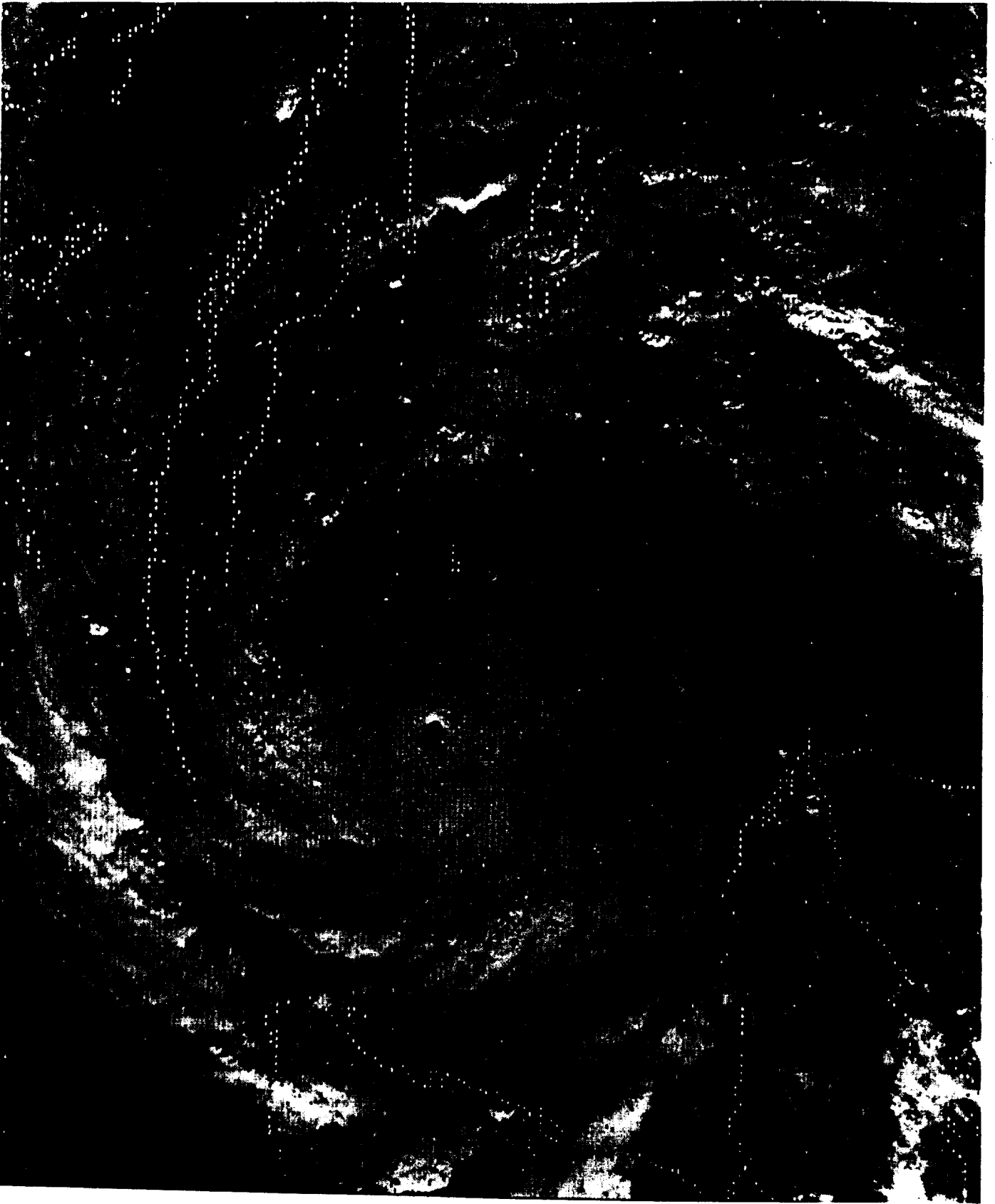
The visible and infrared images collected from the NOAA GOES and TIROS satellites provides forecasters with an essential means of monitoring the development of hurricanes and their future motion. This capability has undoubtedly contributed to the significant reduction of the loss of lives since the 1950's. An example of the view offered by such satellite systems is illustrated in Figure 5, which shows an instantaneous view of a hurricane making landfall near the Yucatan peninsula. This type of image gives a synoptic view of the storm, which yields information on the size and relative strength of the storm. Other critical details, such as accurate measurements of surface winds are not evident in the images. These measurements will require microwave remote sensing because of the ability to penetrate weather and infer wind speed from measurements of sea state.

Because of the need for wind speed and other descriptive data that is needed to support hurricane research activities, an aircraft program is supported to provide data in connection with well defined scientific experiments. These experiments are described each year in a Hurricane Field Program Plan, which is drafted each year prior to the hurricane season by the NOAA Atlantic Oceanographic and Meteorological Laboratory (AOML). For 1992, these experiments have consisted of:

- Hurricane Synoptic - Flow Experiment
- Vortex Dynamics Experiment
- Inner Core Structure and Evolution Experiment
- Clouds and Climate
- Electrification of Hurricane Convection
- Subcloud-Layer Inflow Dynamics of Tropical Cyclones
- Hurricane Landfall Program

The implementation of these experiments requires measurements such as temperature, pressure-height, relative humidity, and most important of all winds. The principal source of data are dropsondes, on-board Doppler radars, and available remote sensing instrumentation. Furthermore, it is desirable to have synoptic measurements available at regular time intervals to study storm evolution and to improve short-term hurricane track position. Of all the instruments mounted on the aircraft, the C-Band Doppler radar comes

2131 13SE88 19A-1 04494 16401 MA19N82W-1



Satellite Image of Hurricane Gilbert (1987) Approaching the Gulf of Mexico
Figure 5

closest to providing a truly synoptic view of the storm. Figure 6 shows a typical microwave image of a hurricane (Gustav) generated by the belly radar, which scans 360° in azimuth. The source of backscatter are rain drops that are confined within the rain bands. The low attenuation due to rain at C-Band makes possible a propagation link that is tens of kilometers, which corresponds to the distances needed to produce a radar image.

Ocean surface probing radars and radiometers simply do not have the range capability of a rain probing radar. In effect, such instruments, even if scanning, will only give data points along the near subtrack of the aircraft as a result of the low altitude relative to the storm dimensions. Figure 7 shows an extended aircraft mission associated with the Vortex Dynamics experiment. This pattern only covers the principal compass directions, and the data are therefore grossly undersampled in the azimuth direction. The only way to increase the sampling density is to place these classes of microwave sensors into low earth orbit.

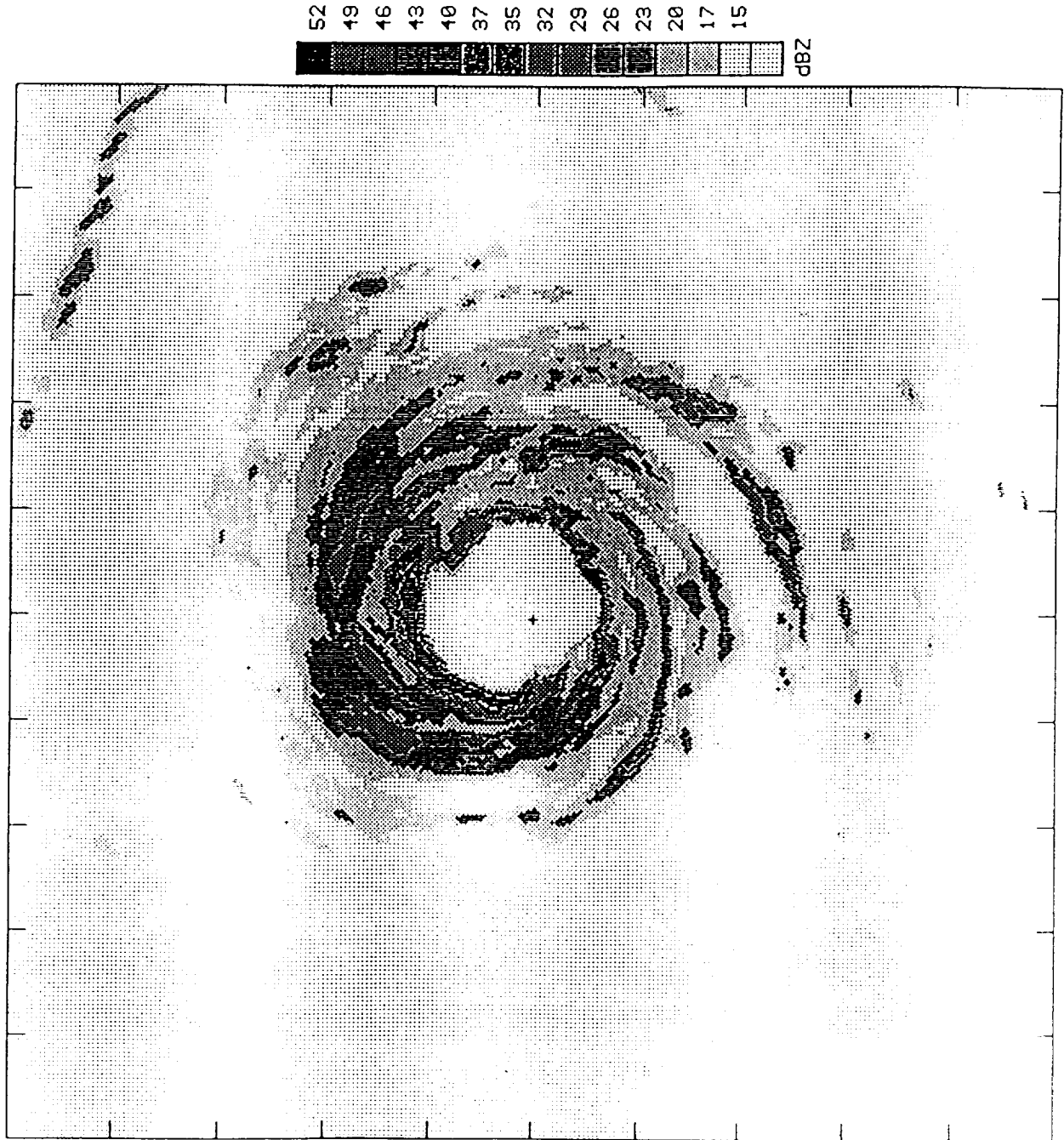
The SEASAT program showed that microwave systems can be a valuable complement for the remote sensing of the earth from space. The continuing disadvantage of passive microwave sensors is their coarse spatial resolution. The spatial resolution achieved by the Electronically Scanned Microwave Radiometer (ESMR) in 1972 was 25 km; the spatial resolution achieved by the Special Sensor Microwave/Imager (SSM/I) in 1987 is also 25 km. The reason that no improvement has occurred over a 15 year time frame relates to antenna size and the choice of orbital altitude. Since these systems use antenna directional patterns to achieve spatial resolution, the best resolution that can be achieved is directly proportional to the antenna size. Therefore, all things being equal, a 5-fold improvement in resolution requires a 5-fold increase in the antenna diameter. The problem is further aggravated if longer microwave wavelengths are required. Historically, spacecraft have been unable to accommodate large antennas proposed for remote sensing experiments. In the first place, mechanical scanning of very large reflectors is difficult. In addition to the momentum compensation required, a point of diminishing returns is reached if a single receiver is used. As the pixel size is reduced, the antenna must be scanned at an increasing rate in order to achieve contiguous imaging. As the spin rate increases, there

900830H1
GUSTAV 3

(min.) (max.)
Pitch= 1.2; 2.0
Roll= -.8; .8
Track= 90.1; 90.5
Drift= -3.6; -2.6
Tilt= 3.4; 3.9
Alt= 2960 m

Rlat= 28.04 N
Rlon= 57.64 W

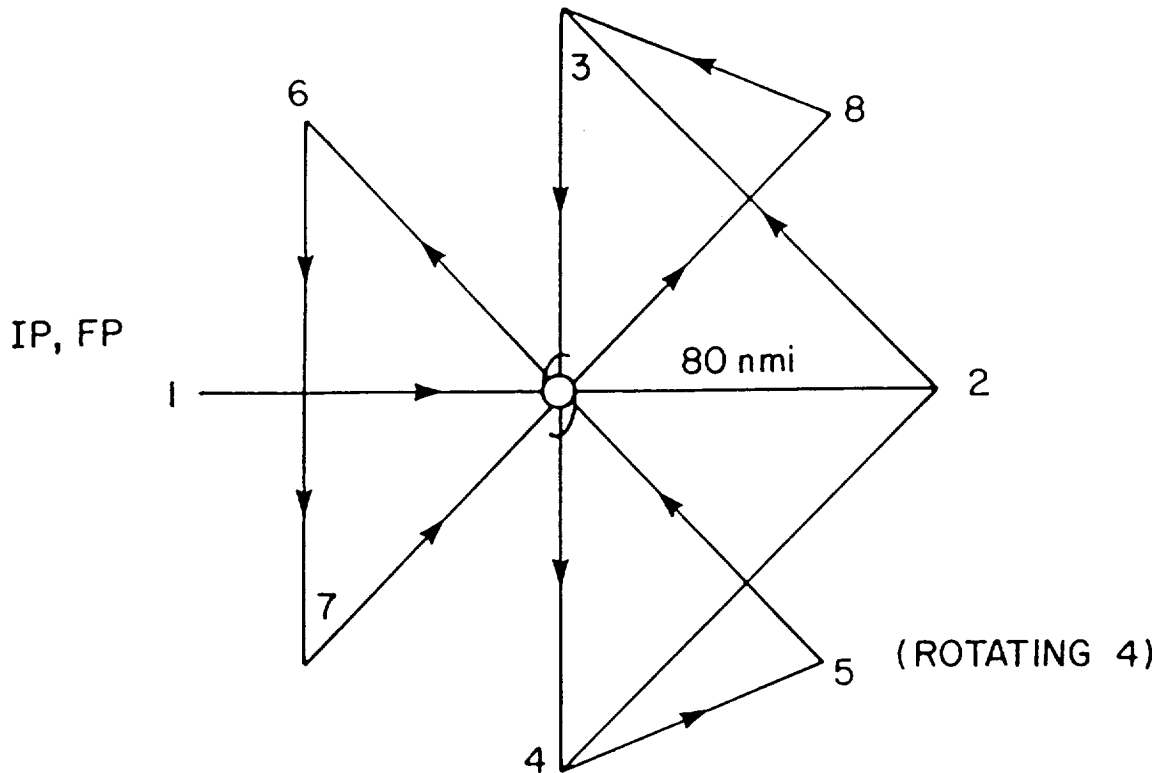
200414 Z
Lower Fuselage
360 X 360 km



Airborne Radar Map of Hurricane Gustav (1991).
Each Division is 36 km.

Figure 6

VORTEX DYNAMICS and ENVIRONMENTAL INTERACTION EXPERIMENT (OPTION 2)



- Note 1. QAO A/C #1 and #2 fly 1-2-3-4-5-6-7-8-3-4-2-1 at 5,000 or 10,000 ft PA.
- Note 2. Each A/C should be at the designated altitude upon reaching the IP and should maintain that altitude until it reaches the FP.
- Note 3. True airspeed calibration is required (Fig. C-1).
- Note 4. The pattern may be entered along any cardinal compass heading.
- Note 5. A/C may attempt to find a wind center on each pass, but should not "hunt" unless directed to do so.
- Note 6. The modified alpha patterns described in the NHOP may be designated as alternatives to the pattern described here.

Vortex Dynamics and Environmental Interaction Experiment (VDEI)/
Option 2, Vortex Evolution: Flight pattern.

Figure 7

will eventually be insufficient pixel dwell to establish integration time needed to develop adequate measurement precision.

Advances in microwave technology over the past decade allow an economical alternative to mechanically scanning a large antenna. In particular, the solid-state GaAs microwave electronics allows systems to be packaged into smaller volumes than other active components used in the past. They draw much less power and can be manufactured in large quantities at a significantly reduced cost. Using monolithic microwave integrated circuit (MMIC) technology it is feasible to fabricate a large number of identical microwave receivers with separate feed horns illuminating a common secondary antenna. These feed horns can be placed to project a multitude of simultaneous beams on the earth surface that are cross-track to the satellite velocity vector. Thus, a microwave image is produced by the forward motion of these cross-track pixels. This technique has been used in optical sensors and is commonly referred to as push-broom scanning. The push-broom method presents two advantages. The imaging process does not require the scanning of a large antenna, and measurement precision is improved with the increased dwell time offered by the multiple receivers.

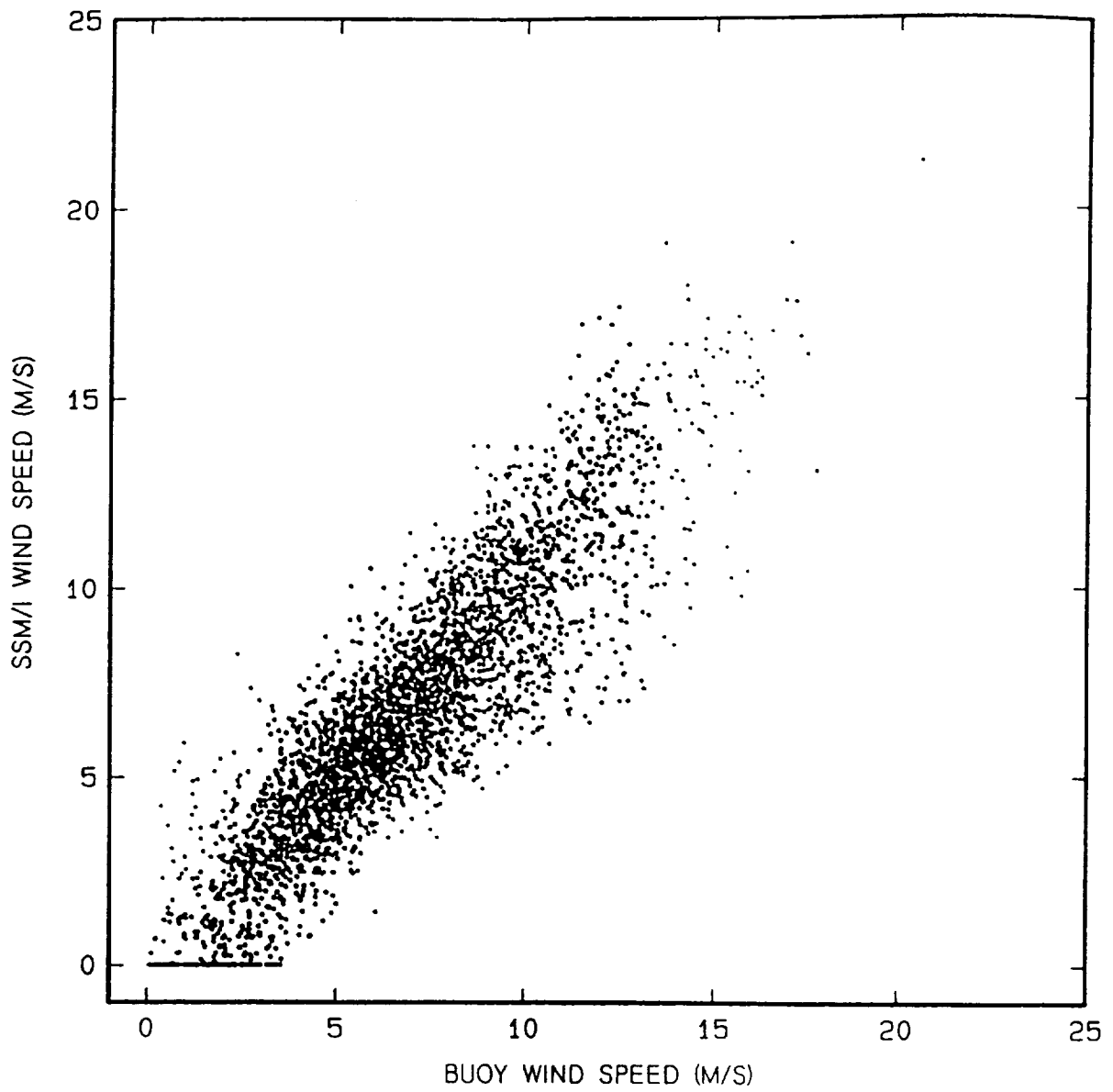
This investigation proposes to develop the Split Window Microwave Radiometer (SWMR) which will utilize a larger antenna than has historically been used. Essentially this will be done by designing the experiment around the spacecraft. That is to say, the SWMR will be considered the prime experiment which will drive the spacecraft and orbital parameters to fit within the Earth Probes Program. The target objective is to provide surface wind speed data through moderate rain and achieve 10 km resolution over a minimum swath that corresponds to the dimensions of the storm. This report will focus on the basic parameters needed to achieve this objective. the remainder of this report will not consider information relevant to weight, volume, packaging, and detailed orbital analyses.

SWMR DESIGN CONSIDERATIONS

Choice of Frequency

The Microwave Remote Sensing Laboratory has spent a great deal of effort validating the performance of the SSM/I with regard to remote sensing of surface winds. While the SSM/I does an excellent job of measuring wind speed in a clear atmosphere [Goodberlet et al., 1990], there are problems retrieving winds in the presence of heavy cloud cover and rain. Indeed, when the rain rate hits a threshold of 1-3 mm/hr, the retrieval accuracy of wind speed exceeds ± 10 m/s, which is far too coarse a measurement to be of value to any user of the wind speed data. The basic problem is that the lowest microwave frequency used by the SSM/I is 19 GHz. For the given size of the antenna (80 cm), the footprint on the ground exceeds 60 km, and the spatial resolution becomes unacceptable. As an example of the performance of the SSM/I, Figure 8 shows a cluster plot of buoy winds and SSM/I derived winds. This plot was generated by pairing a year's worth of data sets with the constraint that the selected SSM/I footprints were located within 25 km of the buoy, and that the measurements were made within one-half hour of each other. Over the windspeed range from 0 to 26 m/s, the data scatter is ± 2 m/s, which was deemed acceptable by the users. This wind speed product has been used since 1987 without complaint by a large number of users. Operationally, about 15%, the data are flagged as unusable as a result of the condensed water burden in the atmosphere. Although this is a small percentage, it is an important percentage, since high winds are usually accompanied by significant precipitation.

Ideally, we would like to collect data at a much lower frequency, preferably C-Band, where we know that accurate wind speed measurements can be made in the presence of heavy rain for all expected wind speeds up to and including hurricane force winds. In practice, we would like to keep the frequency as high as possible to achieve the best possible spatial resolution. Obviously, there are competing requirements, so that a compromise is needed. In order to illustrate the effects of the rain attenuation, we consider the theoretical value of the brightness temperature observed by an upward-looking instrument. With no background radiation, the appropriate expression is:



Buoy vs. SSM/I Winds
Figure 8

$$T_B = T_M(1 - e^{-\tau \sec \theta_o}) \quad (1)$$

where T_M is the mean atmospheric temperature in Kelvins, θ_o is the viewing angle as measured from nadir, and τ is the atmospheric opacity. The empirical relationship between opacity, frequency f and rain rate R is given by:

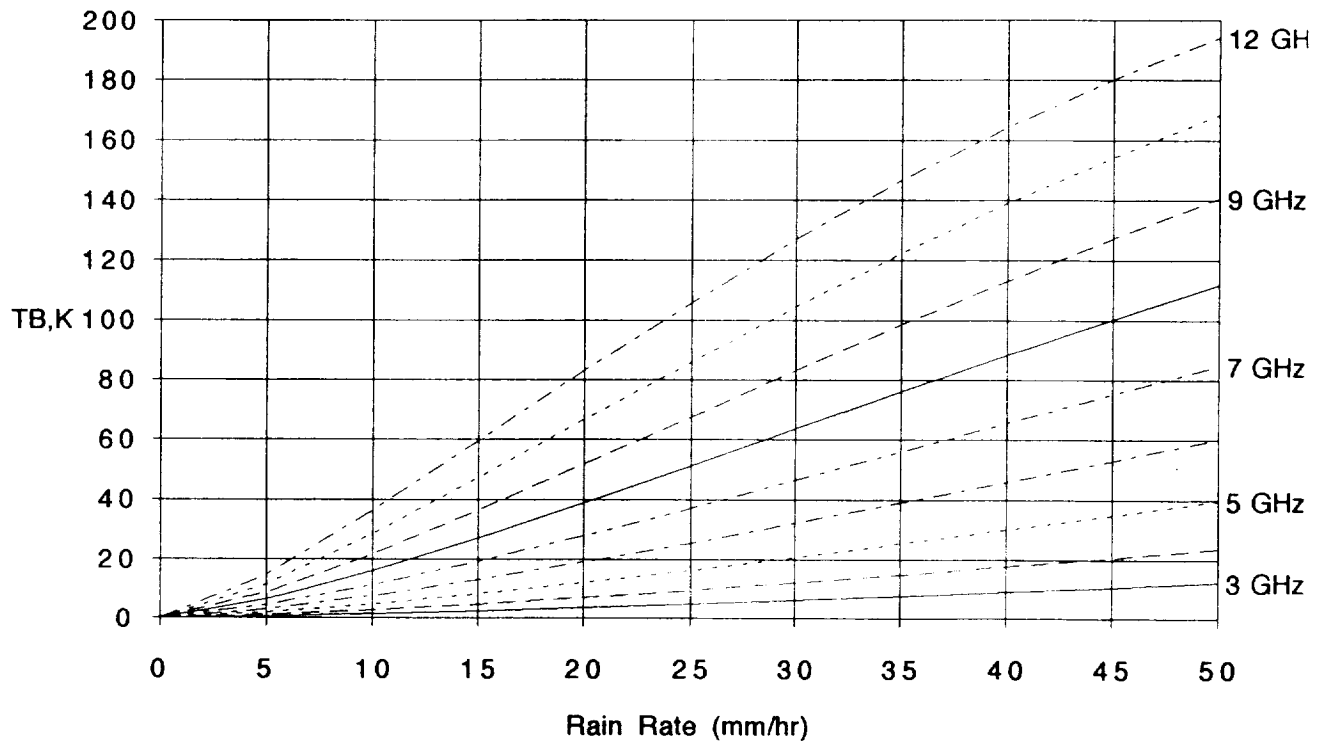
$$\tau = 3.74(0.01f)^3 R^{1.35} \quad (2)$$

where f is in GHz and R is mm/hr. Figure 9 shows a plot of brightness temperature vs. rain rate with frequency as a parameter and varying from 3 GHz to 12 GHz at a viewing angle of 50°. Note that the brightness temperature increases with increasing rain rate and frequency as implied by equation (2). Our experience with the SSM/I is that when the excess brightness temperature expressed by equation (1) exceeds 60K, the accuracy of the surface retrievals are severely compromised as a result of two way attenuation experienced by a downward looking geometry and the need for good radiometric accuracy necessary to produce accurate wind speed measurements. Therefore, in order to meet this threshold, C-Band is needed to produce accurate wind speed retrievals over the entire range of rain rates up to 50 mm/hr. However, if we choose to design the system to produce retrieval at a lower rain rate threshold, say 15 mm/hr., then we are granted some leeway regarding the choice of the maximum usable frequency.

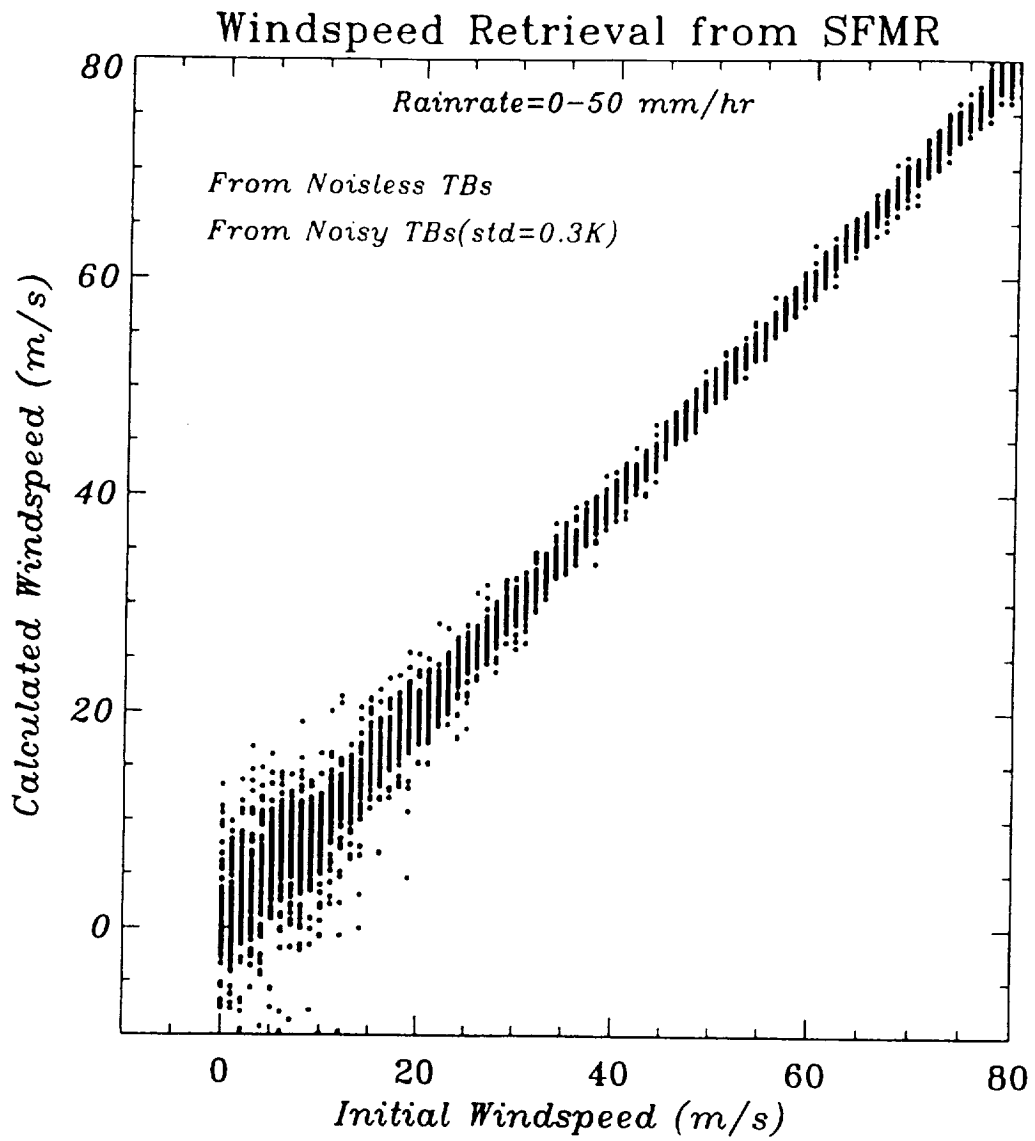
Another way of looking at the surface wind retrieval problem in the presence of rain is to consider retrievals obtained with a noiseless instrument vs. one with a realistic noise performance. The inference here is that perfect surface retrievals can be achieved with a perfect noise-free instrument. An example using C-Band is shown in Figure 10. This is a simulation based upon the actual noise level of the SFMR and the actual frequencies used in flight. This curve shows the amount of error expected in the wind speed retrieval when the noise level is 0.3K. The resultant error is approximately 2 m/s for wind speeds higher than 20 m/s. Reduced accuracy is evident for wind speeds below 20 m/s because of some reduced sensitivity at C-Band and at nadir. Figure 11 shows a similar plot for an algorithm that uses higher frequencies (8-10 GHz) and a reduced range of rain rates.

Rain Signature.

Brightness Temperature vs Rain Rate

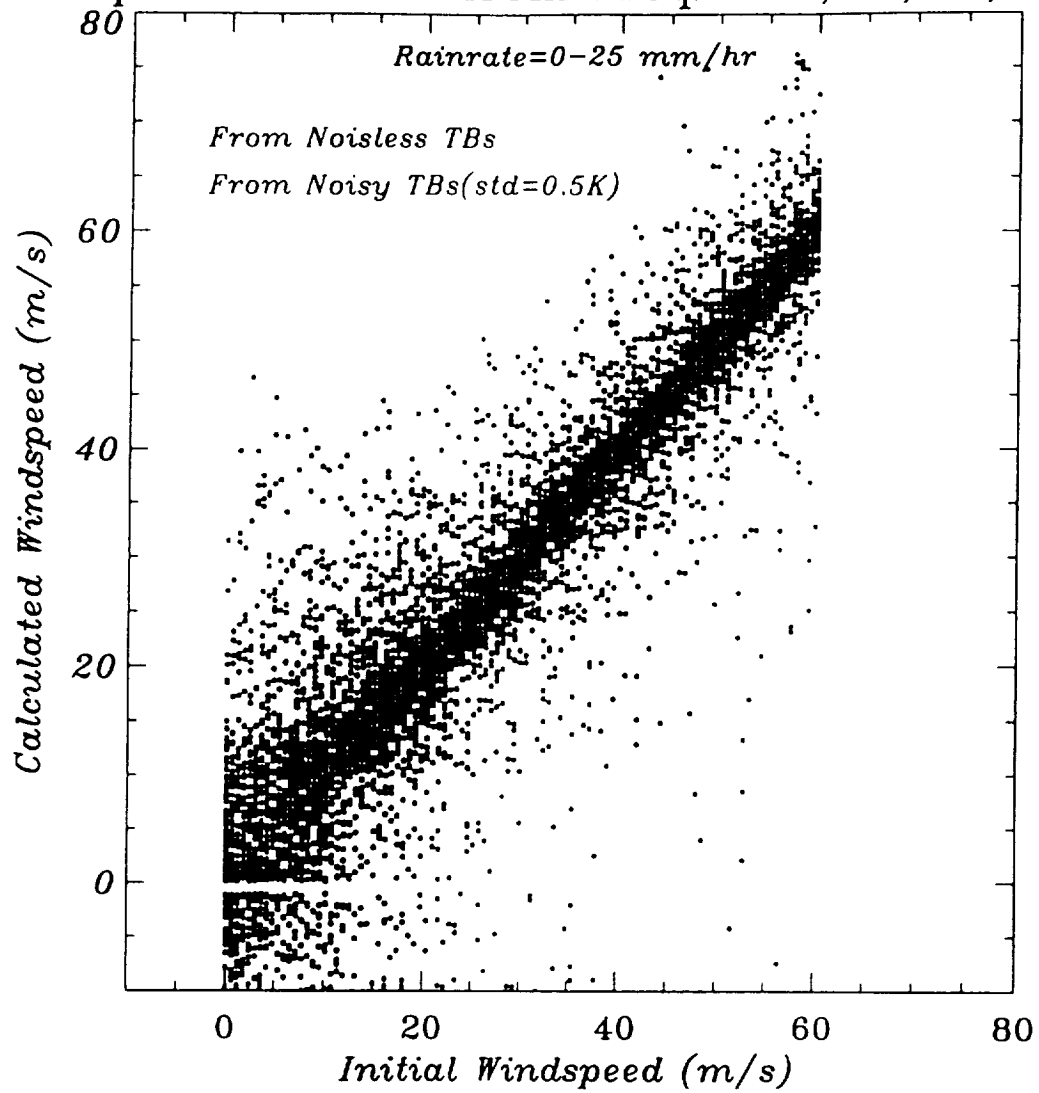


Brightness temperature vs. rain rate for upward-looking radiometer. Frequency is a parameter
Figure 9



C-Band retrieval windspeed with 0.3K instrument noise
Figure 10

Windspeed Retrieval from Freqs. 8.0,8.5,9.0,9.5,10.0



Wind speed retrieval using X-Band frequencies with 0.5K instrument noise level
Figure 11

Although the scatter is greater, the curve nevertheless indicates that a wind speed retrieval is possible at a somewhat reduced accuracy.

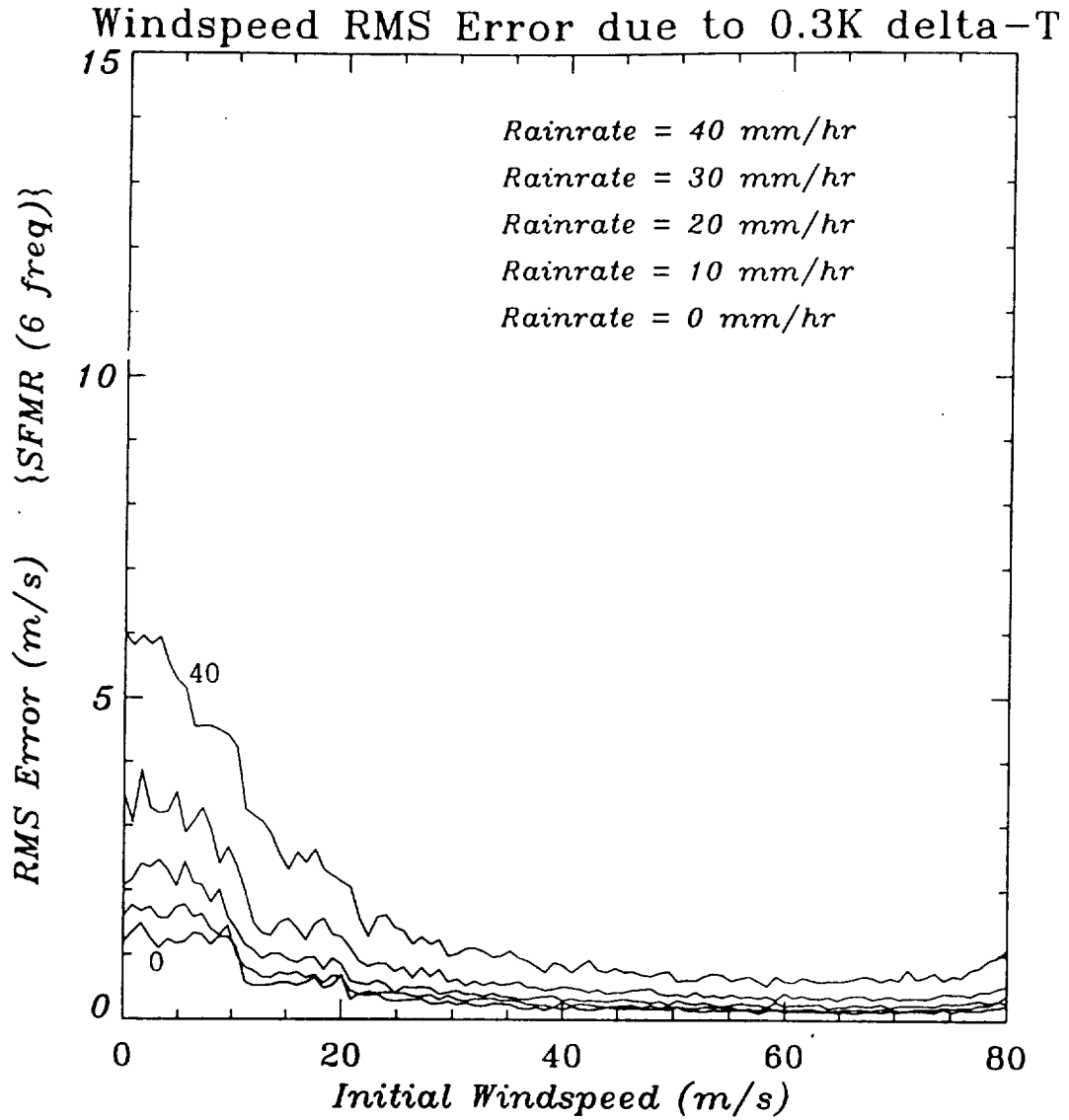
A better way of presenting the data is to plot rms error in the wind speed retrieval vs. average wind speed with rain rate as a parameter. This is done first for the retrieval based upon the SFMR winds, and the results are shown in Figure 12. These results generally confirm the scatter plot shown previously in Figure 10. That is to say, accuracies better than ± 2 m/s are achieved at the higher wind speeds, regardless of the amount of rain between the surface and the down-looking radiometer. It is of further interest to note that high rain rates tend to reduce the accuracy of the wind speed retrieval at the lower wind speeds. Since heavy rain fall is usually associated with high winds, this particular distribution of errors is fortuitous. In other words, we expect to see light rain coupled with areas of low wind speed, thereby resulting in a more uniform retrieval error. Figure 12 also clearly indicates that C-Band is ideal, provided a large enough antenna can be accommodated by the spacecraft.

Figure 13 shows how the errors drastically change when the electromagnetic frequency is increased by about a factor of two. Here we see that the errors associated with rain rates of 50 mm/hr are off scale, and that rain rates as low as 20 mm/hr. are an obvious threshold for retrieving useful data. Note that the instrument precision (ΔT) here is 0.5K. Figure 14 shows how the results further deteriorate when the ΔT increases to 1.0K.

Figure 6 is a helpful indicator for determining to what degree a 20 mm/hr threshold in rain rate will obscure the ocean surface for reliable wind speed measurements. This figure defines Hurricane Gustav in terms of C-Band radar reflectivity. The grey levels in this image are renditions of a radar parameter called "dBZ". The parameter Z was defined by Marshall and Palmer [1948] and is given by

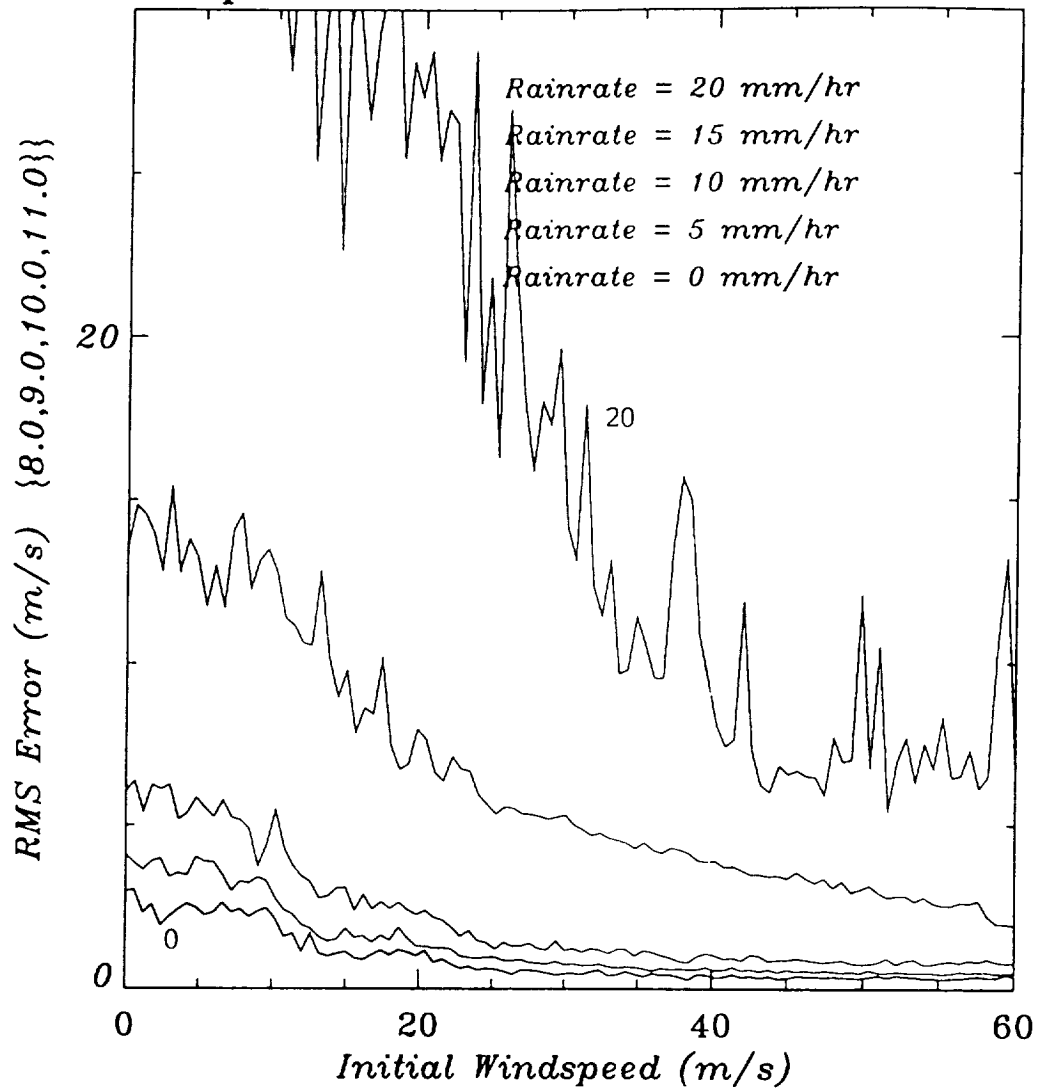
$$dBZ = 10 \log(200R^{1.6}) \quad (3)$$

for $f < 10$ GHz. Again R is the rain rate. A rain rate of 20 mm/hr therefore corresponds to a dBZ of 43.8. Therefore, most of the storm, except for the extreme dark shades of grey will successfully be probed by a measurement whose rain rate threshold is 20 mm/hr. In



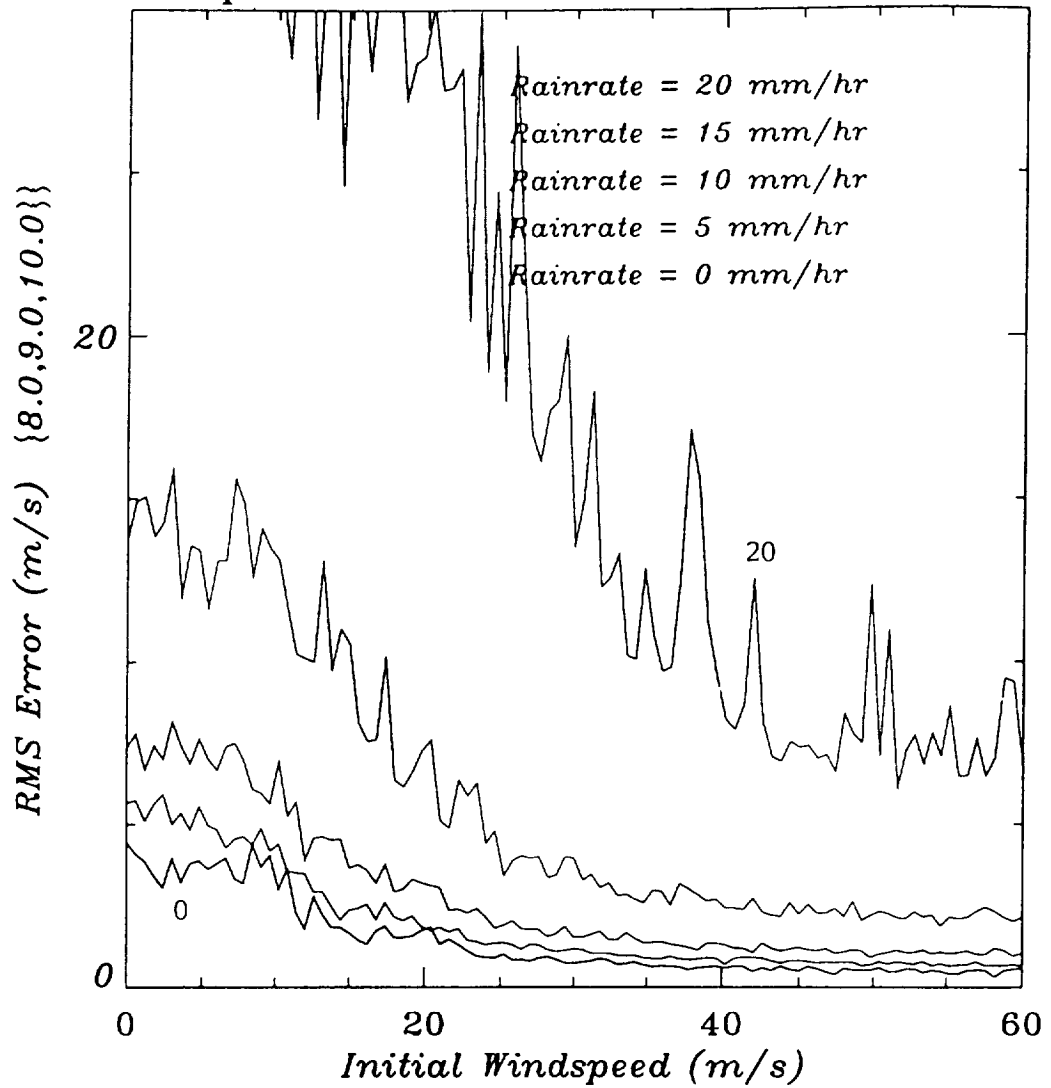
RMS retrieved wind speed error for the C-Band SFMR. The instrument noise level is 0.3K
 Figure 12

Windspeed RMS Error due to 0.5K delta-T



RMS retrieval error using X-Band frequencies with a 0.5K instrument noise level
Figure 13

Windspeed RMS Error due to 0.5K delta-T



RMS retrieval error using X-Band frequencies with a 0.5K instrument noise level. This is the same as Figure 13, except the upper X-Band frequency has been dropped

Figure 14

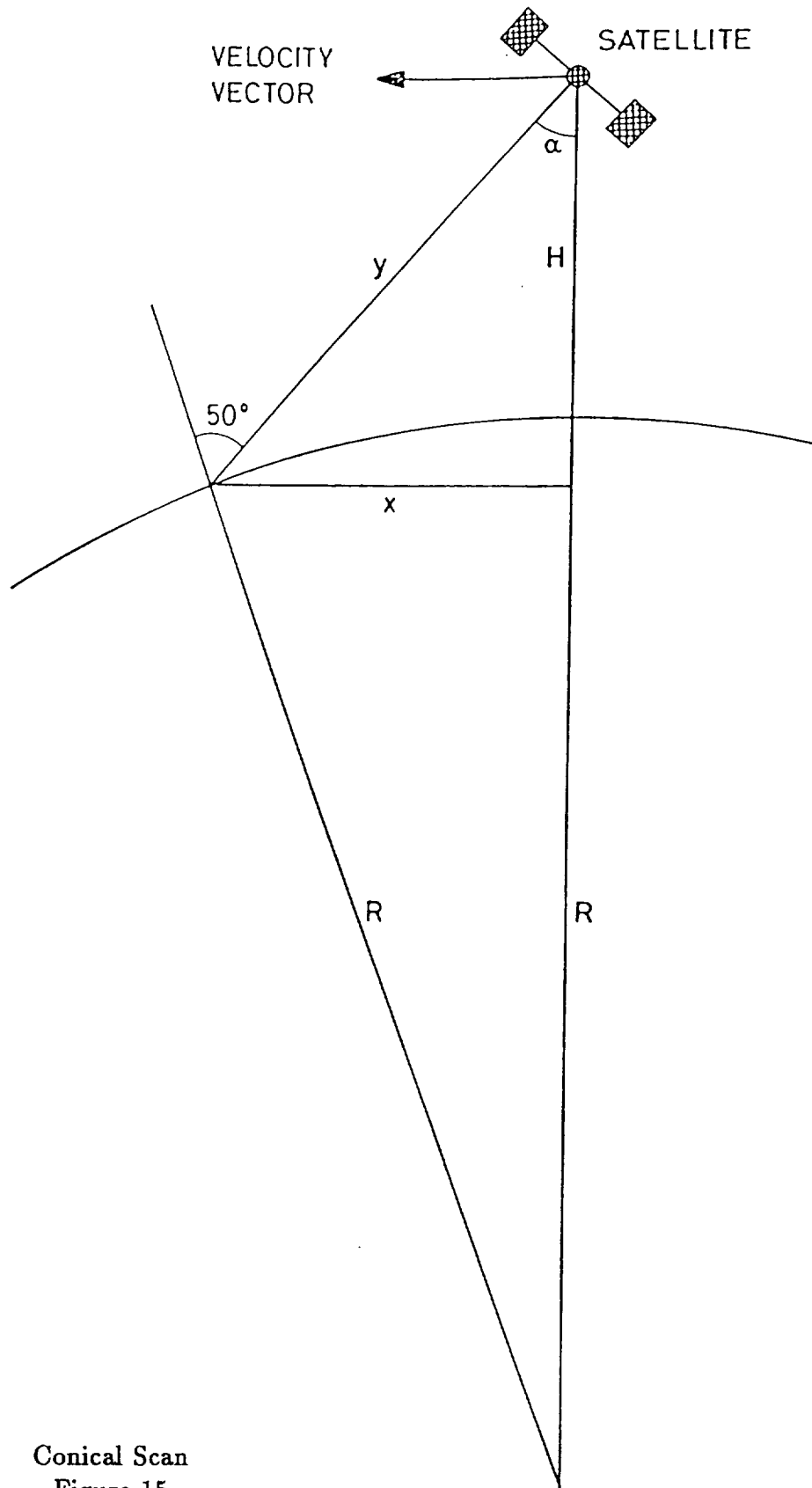
addition, if the spatial resolution is 10 km or greater (approximately 1/3 of a division of the grid in Figure 6), the radiometer will observe rain rates whose average value is smaller than that resolved by the aircraft radar.

SPACECRAFT CONSIDERATIONS

A sketch of the geometry of a spacecraft scanning antenna is shown in Figure 15. In this Figure, R is the radius of the earth, H is the spacecraft altitude, Y is the slant range to a given point on the earth, and X is the cross range. Most spacecraft radiometers are designed to keep the local angle of incidence fixed, which means that the slant range Y and therefore spatial resolution remains constant as a function of scan angle. The specific choice of the a variable angle of incidence (usually 50°) determines X and therefore the width of the data swath. The problem with the conical scan is that the slant range is approximately twice the spacecraft altitude, which degrades resolution since spatial resolution is directly proportional to slant range. One way of improving spatial resolution is to do cross-track scanning. This has the disadvantage of introducing a variable footprint and angle of incidence; however, other previous systems (e.g. ESMR, KRMS and a Canadian radiometer) have been able to work around the distortions that are caused by these two effects. We will therefore assume that the SWMR will accommodate a cross-track scanning pattern.

The purpose of this study is to develop the first-order analysis needed to develop the system requirements. As these numbers were generated, it is clear that more detailed analyses are needed to further converge on an acceptable antenna design and receiver configuration. In developing these numbers, the following equations were used:

- Antenna beamwidth: $\theta_B = 1.2\lambda/D$ where λ is the electromagnetic wavelength and D is the antenna diameter.
- Footprint diameter at nadir: $FPS = H\theta_B$ where H is the spacecraft altitudes.
- Footprint diameter at scan edge: $FPL = \frac{FPS}{\cos^2 \alpha}$ where 2α is the swath sector.
- Data swath: $S = 2H \tan \alpha$.
- Spacecraft velocity $v_s = \sqrt{gR^2/(R + H)}$ where g is acceleration due to gravity.
- Dwell time needed per pixel for a single receiver connected to the antenna: $T_D = (FPS)(FPL)/v_s S$.
- Radiometer Precision: $\Delta T = \frac{T_A + T_{sys}}{\sqrt{BT_D}}$.



Conical Scan
Figure 15

where T_A is the scene temperature, T_{sys} is the system noise temperature and B is the receiver bandwidth. We will assume $T_A = 300K$, $T_{sys} = 600K$ and $B = 100MHz$.

Table I gives an example of the size of the earth - located antenna footprint and system ΔT as a function of antenna diameter. The assumed altitude is 300 km and the swath width is 600 km, which corresponds to a field of view of 90° . This Table shows that a 10 km spatial resolution is achieved with an antenna having an aperture size of 2 m. The ΔT of 0.79K of a single scanning receiver can be reduced to approximately 0.5K by spoiling the resolution in the cross-track scan direction. This would have the added benefit of producing a square pixel for better image fidelity. The antenna size requirements will of course vary as the orbital parameters are changed. For example, a 600 km altitude will require a 4m diameter antenna in order to achieve the same resolution requirements.

Table I
SWMR Design Parameters

ORBITII

H(KM)	300.00		
R(KM)	6000.00		
F(GHZ)	10.00		
ALPHA(DEG)	45.00		
VS(KM/S)	7.48		
S(KM)	600.00		
Pi	3.14		
D(M)	FPS	FPL	ΔT
1.00	10.80	21.60	0.39
1.25	8.64	17.28	0.49
1.50	7.20	14.40	0.59
1.75	6.17	12.34	0.69
2.00	5.40	10.80	0.79
2.25	4.80	9.60	0.89
2.50	4.32	8.64	0.99
2.75	3.93	7.85	1.09
3.00	3.60	7.20	1.18

Antenna Consideration

A SWMR placed in low earth orbit (approximately 300 km altitude) will require an aperture of approximately 2 m to achieve 10 km spatial resolution at X-Band. In addition to developing this spatial resolution, the antenna must be capable of developing cross-track scan, and must operate over a range of frequencies in the 8-12 GHz band. The type of antennas that appear to be suitable are the parabolic torus, the electronically scanned phased array with a corporate feed to achieve bandwidth, and the lens antenna that has seen some development by Grumman aircraft. We tend to favor the Grumman concept because of the difficulty in packaging reflector antennas, and the losses and packaging problems associated with the electronically scanned phase array. The packaging is an important design element if we wish to launch the SWMR on a relatively small launching system.

The geometry that is appropriate for the analysis of the lens antenna is shown in Figure 16. Although the lens antenna is drawn as a flat plate, it consists of an array of discrete passive elements that effectively adds a segment of transmission line whose length depends upon distance from the center of the lens. For example, if we choose the length of line that depends upon the square of the distance, then a focal point is created a distance f above the array. A spherical wave front produced by a feed placed at f will therefore become a plane wave front after transmitting through the lens, and the effective aperture corresponding to the size of the lens. To show this, let the path length through the lens be given by the following formula:

$$\ell = -\frac{y^2}{2f} - f \quad (4)$$

If the feed is displaced a distance δ from the y -axis, as shown in the figure, then the phase ϕ of the wave that propagates from the feed and through the lens is given by:

$$\phi = \frac{2\pi}{\lambda} \left[\sqrt{f^2 + (y - \delta)^2} - \frac{y^2}{2f} - f \right] \quad (5)$$

And if the focal length is large, such that $f \gg y$, then a series expansion of (5) results in

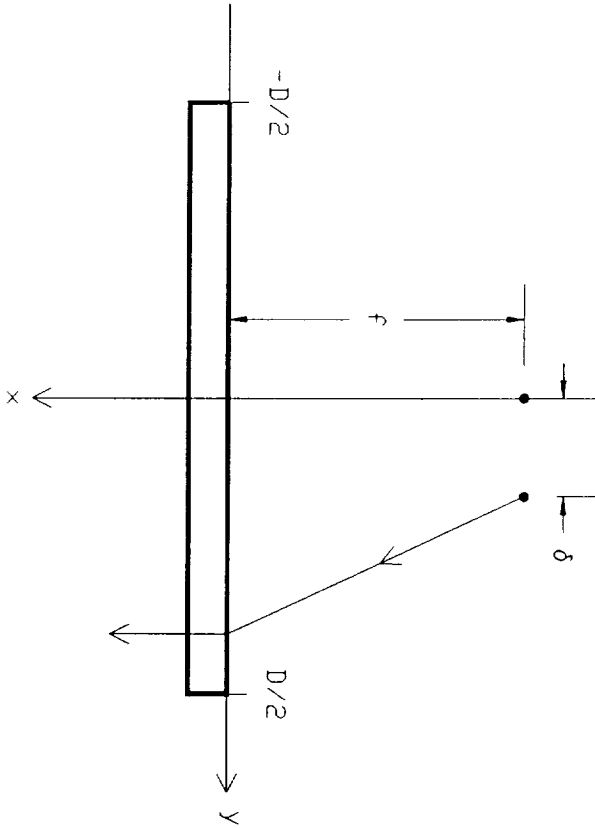


Figure 16. Geometry of lens antenna with feed place at a distance, f , above the lens.

$$\phi \cong \frac{\pi\delta^2}{\lambda f} - \frac{2\pi\sigma y}{\lambda f} \quad (6)$$

The lens therefore converts a quadratic phase variation to a linear one. The elimination of the quadratic error causes a narrowing of the beam and the linear term results in one-dimensional scanning, which is one of our objectives. To illustrate the implementation of the scan, we note that the far field is Fourier transform of the field distribution over the aperture of the lens; i.e.,

$$E(\theta) = \int_{-D/2}^{D/2} A(y)e^{-j\frac{2\pi y}{\lambda} \sin \theta} dy \quad (7)$$

where $A(y)$ is the complex field distribution over the aperture, θ is the scan angle, and D is the dimension of the lens. With $A(y) = e^{j\phi}$, equation (7) integrates to the following:

$$|E^2(\theta)| = \frac{\sin^2 \left[\frac{\pi D}{\lambda} (\sin \theta - \delta/f) \right]}{\left[\frac{\pi D}{\lambda} (\sin \theta - \delta/f) \right]^2} \quad (8)$$

If we identify δ/f as $\sin \theta_o$, where θ_o is the scan angle, then we see that cross-track scanning is accommodated by moving the feed. This can be done either by mechanical displacement of a single receiving horn or by an off-set positioning of a switchable feed array or by using multiple receivers. We are not that familiar with the design of lens antennas, but it would seem that scanning could also be accommodated by electrically altering the line length as represented by equation 4.

Summary and Recommendations

In this report, we have discussed the need for a Split Window Microwave Radiometer (SWMR) to monitor tropical storms and hurricanes. Although there are science issues involved in the study of storm genesis and evolution, the main driver for such a system involves better definition of land fall for hurricanes. The SWMR concept is sound, since it is based upon a successful C-Band airborne sensor that has reliably provided remote sensing

measurements of surface winds through heavy rain fall since 1984. The only disadvantage of the present concept is that C-Band will require large antennas to achieve 10 km spatial resolution from low earth orbit.

In order to reduce the antenna size requirement, a study was done to determine if the frequency can be increased without seriously compromising the ability of the instrument to measure surface winds in the presence of moderate rain. Our study has concluded that the frequency can be increased to X-Band and still penetrate rain fall rates as heavy as 20 mm/hr. By increasing the electromagnetic frequency by a factor of 2, the acceptable antenna aperture dimension becomes 2 m at 300 km altitude, which does not seem to be unreasonable in size. One attractive antenna configuration will be the lens antenna with a feed or several feeds positioned at the focal plane.

It would seem that the next stage would be to initiate more critical engineering definition studies. These studies would result in defining an acceptable orbit, and an acceptable spacecraft design including the instrument and the type of bus that is needed to support sensor operation and data retrieval. Such a system design is needed in order to determine the minimum launch system that is needed to place the SWMR into low earth's orbit.

References

- [1] Nordberg, W., et al., 1971. Measurements of Microwave Emissions from a Foam-Covered, Wind-Driven Sea, *J. Atmos. Sc.*, Vol. 38, pp. 428-435.
- [2] Ross, D.B., and Cardone, V., 1974. Observations of oceanic Whitecaps and Their Relation to Remote Measurements of Surface Wind Speed, *J. Geophys Res.*, Vol. 79, No. 3, pp. 444-452.
- [3] Hollinger, J.P. 1971. Passive Microwave Measurements of Sea Surface Roughness. *IEEE Trans. Geosci. Electro.*, Vol. GE-9, No. 3, pp. 165-169.
- [4] Webster, W.J., et al., 1976. Spectral Characteristics of the Microwave Emissions From a Wind-Driven Foam-covered Sea. *Geophys Res.*, Vol. 81, No. 18, pp.3095-3099.
- [5] Harrington, R.F., 1980. The Development of a Stepped Frequency Microwave Radiometer and its Application to Remote Sensing of the Earth, NASA TM-81847, LaRC.
- [6] Lawrence, R.W., et al., 1986. Design and Development of a Multibeam 1.4 GHz Pushbroom Microwave Radiometer, NASA TM-89005, LaRC.
- [7] Jones, W.L., Black, P.G., Delnore, V.E., and Swift, C.T., 1981. Airborne Microwave Remote Sensing Measurements of Hurricane Allen, *Science*, Vol. 214, pp.274-280.
- [8] Black, P.G., and Swift, C.T., 1984. Airborne Stepped Frequency Microwave Radiometer Measurements of Rainfall Rate and Surface Wind Speed in Hurricanes, 22nd Conf on Radar Meteorology, 10-13 Sept. 1984, Zurich, Switzerland, AMS pub.
- [9] Tanner, A., Swift, C.T., and Black, P.G., 1987. Operational Airborne Remote Sensing of Wind Speeds in Hurricanes, 17th conf on Hurricanes and Tropical meteorology - AMS, Miami, FL, pp. 385-387.
- [10] Goodberlet, M.A., Swift, C.T., and Wilkerson, J.C., 1989. Remote Sensing of Ocean Surface Winds with the Speed Sensor Microwave/Imager, *J. Geophys. Res.*, Vol. 94(C10), pp. 14,547-14,555.
- [11] Marshall, J.S., and Palmer, W.McK., 1948. The Distribution of Raindrops with Size, *J. Meteorol.*, Vol. 9, pp.322-325.